Hole growth in freely standing polystyrene films probed using a differential pressure experiment

C. B. Roth and J. R. Dutcher
Department of Physics and the Guelph-Waterloo Physics Institute, University of Guelph, Guelph, Ontario, Canada N1G 2W1
(Received 16 July 2004; revised manuscript received 19 April 2005; published 10 August 2005)

We have probed the whole chain mobility of polymer molecules confined to freely standing films by measuring the flow of gas through holes growing in the films at elevated temperatures using a differential pressure experiment. Freely standing polystyrene films were measured for the temperature range 92 °C$<T<$105 °C for films with two different molecular weights $M_w=717\times10^3$ and 2240×10^3, with thicknesses 51 nm$<h<$97 nm. This range of film thicknesses is of particular interest because large reductions in the glass transition temperature T_g have been measured previously for freely standing PS films in this thickness range. We find that hole formation and growth, and therefore substantial chain mobility, does not occur until temperatures close to the bulk value of the glass transition temperature T_g^{bulk}. The characteristic growth times τ for the thinnest films, which have reduced values of T_g, are not substantially less than those for thicker films, and we find that these small differences in τ can be understood in terms of the bulk phenomenon of shear thinning. We also show that the viscosity at the edge of the hole inferred from the characteristic growth times obtained in this and previous studies exhibit shear thinning with reduced shear strain rates β that span twelve orders of magnitude.

DOI: 10.1103/PhysRevE.72.021803 PACS number(s): 68.15.+e, 68.60.Dv, 83.60.Fg

I. INTRODUCTION

The study of polymer molecules in confined geometries provides a means of probing polymer-surface interactions, as well as the effect of confinement on the motion of the molecules on different length scales, ranging from the segment size to the overall size of the polymer molecules. During the past decade, substantial experimental, theoretical, and computational research on polymers confined to thin films, for which strong substrate interactions can be neglected, has indicated that mobility on the segmental length scale is increased as the film thickness h is decreased, as measured by reductions in the glass transition temperature T_g [1,2]. The decrease in T_g with decreasing h is particularly striking for freely standing films of polystyrene (PS) which exhibit reductions in T_g by as much as 70 °C for $h\approx30$ nm and $M_w=1.25\times10^6$ [3–6]. Similar reductions in T_g with decreasing h for freely standing films of poly(methyl methacrylate) (PMMA) have also been observed recently, however, the magnitude of the reductions in T_g are not as large as that measured for PS films [7].

Mobility on the length scale of the entire chain has been studied both by diffusion of entire chains [8–14] and the growth of holes in both supported [15–23] and freely standing [24–29] polymer films. Diffusion studies involving the diffusion of fluorescently tagged chains [8] and probe dye molecules [30,31], the interdiffusion between deuterated and nondeuterated polymer layers [9–14], and the adhesion of two interfaces in contact [32] indicate that either the mobility of entire chains is not enhanced substantially compared with that in the bulk [8,13,14,32], or it is reduced [9–12,31].

At temperatures comparable to or greater than the glass transition temperature in bulk, T_g^{bulk}, thin polymer films can be susceptible to the formation and growth of holes if there is an attractive dispersion interaction acting across the film thickness. This is always true for freely standing polymer films, because of symmetry with respect to the midplane of the film [33]. An attractive dispersion interaction is frequently obtained for polymer films supported on underlying substrates, and the subsequent breakup or dewetting of supported polymer films has been studied extensively [15–23]. Holes can form in the films either spontaneously, through amplification of thermal fluctuations of the film interfaces, or through nucleation at defects. The formation of a hole is driven by the attractive dispersion interaction acting across the film thickness which has to overcome the increase in free energy due to the creation of new surface as specified by surface tension. For a nucleated hole to grow with time, it must exceed a critical radius $R_c=h/2$ [34]. Once a sufficiently large hole forms, its growth is driven by surface tension acting at the edge of the hole and limited by viscous damping within the film. For a thin, freely standing viscous film, the radius R of a hole is observed to grow exponentially with time t [24,26,29]:

$$R(t)=R_0\exp(t/\tau), \tag{1}$$

where R_0 is the radius at $t=0$, and τ is the characteristic growth time that can be written as

$$\tau=\eta h/\epsilon, \tag{2}$$

where η is the viscosity at the edge of the hole and ϵ is the surface tension.

Although hole growth in thin polymer films provides a unique probe of the whole chain mobility, since chains have to move for the hole to grow, it is more complicated than the chain diffusion measurement because the flow is driven by surface tension. The driven flow produces shear strain rates $\dot{\gamma}$ given by [26,29]

$$\dot{\gamma} = 2/\tau. \quad (3)$$

At temperatures that are large compared with T_g^{bulk}, the polymer can be treated as a simple viscous liquid [18,19,24–26]. Hole growth in freely standing films of polydimethylsiloxane (PDMS) has been measured by Debrégeas *et al.* at room temperature ($T_g = -123$ °C for PDMS of $M_w = 308 \times 10^3$) and the hole radius was observed to grow exponentially with time, with uniform thickening of the films and the absence of a rim at the edge of the hole [24,25].

At lower temperatures relative to T_g^{bulk}, corresponding to much higher viscosities, the analysis of the hole growth experiment can become more complicated because of the importance of nonlinear viscoelastic effects such as shear thinning [35,36]. The phenomenon of shear thinning describes a power law decrease in viscosity η with increasing shear strain rate $\dot{\gamma}$ which can be observed in polymers and other complex systems [37–41]. For small shear rates, the viscosity is equal to the constant zero shear rate viscosity η_0, whereas for $\dot{\gamma}$ values greater than some critical value $\dot{\gamma}_{\text{cr}}$

$$\eta(\dot{\gamma}) = \eta_0 \left(\frac{\dot{\gamma}_{\text{cr}}}{\dot{\gamma}} \right)^d, \quad (4)$$

where the power law exponent d is typically ~ 0.8. It has been observed that the power law decrease in η with increasing $\dot{\gamma}$ was only observed for molecular weight M_w values greater than a critical molecular weight M_c, which coincided with the crossover behavior in η_0 from a linear molecular weight dependence to $\eta_0 \sim M_w^{3.4}$ [42]. Also, Stratton showed that for a series of monodisperse polystyrene (PS) melts, with M_w's ranging from 117×10^3 to 242×10^3, the $\eta(\dot{\gamma})$ values were independent of M_w in the nonlinear viscosity regime [43]. Stratton reasoned that since the viscosity is dominated by the effects of entanglements in this M_w regime, one interpretation for the M_w independence of $\eta(\dot{\gamma})$ was that the various samples all had the same number of effective entanglements at a given value of $\dot{\gamma}$.

Hole growth measurements were performed on freely standing PS films of $M_w = 767 \times 10^3$ at a relatively high temperature of $T = 115$ °C [26], which was 18 °C greater than the bulk value of the glass transition temperature $T_g^{\text{bulk}} = 97$ °C. Exponential growth of the hole radius was also observed for the freely standing PS films which was consistent with treating the polymer as a highly viscous liquid undergoing the bulk phenomenon of shear thinning.

At even lower temperatures relative to T_g^{bulk}, more complex behavior is observed. In hole growth measurements of PS films supported on a thin layer of PDMS at temperatures close to T_g^{bulk} of PS [20–23], an asymmetric rim was observed that was not previously observed in liquid films. The shape of the asymmetric rim can be accounted for theoretically by the shear thinning mechanism [44–46] and viscoelastic effects [47]. Recently, a transition from linear to exponential growth of the hole radius was observed during the growth of holes in freely standing PS films at temperatures very close to T_g^{bulk} [29]. Excellent fits to the $R(t)$ data were obtained by allowing for a time-dependent viscosity, characterized by a transient behavior that decayed exponentially with time that was attributed to the disentanglement of chains via the convective constraint release (CCR) mechanism of the tube theory for entangled polymer dynamics [48]. Additionally, in measurements by Xavier *et al.* of freely standing PS films with thickness $h = 6$ μm, exponential growth was observed at an elevated temperature of $T = 136$ °C with τ values that are consistent with the zero shear rate viscosity η_0 values of the bulk material, and linear growth was observed at temperatures close to T_g^{bulk} for films with thickness $h = 80$ nm [28].

In the present manuscript, we describe measurements of hole growth in freely standing PS films of different thicknesses and molecular weights at temperatures both above and below T_g^{bulk} using a custom-built differential pressure experiment (DPE) [27]. In the DPE, the flow of gas through the holes in the film is measured which allows the determination of the characteristic growth time τ of the holes. In particular, we have measured τ as a function of temperature T for relatively thick films with $h \approx 95$ nm for which the T_g value is equal to that in bulk, as well as for relatively thin films with h as small as 51 nm for which the T_g value is reduced by 70 °C from the bulk value. Only small shifts in the $\tau(T)$ data were observed with decreasing thickness h, which can be explained quantitatively by the bulk phenomenon of shear thinning.

II. EXPERIMENT

Monodisperse PS of two different molecular weights $M_w = 717 \times 10^3$ ($M_w/M_n = 1.12$) and $M_w = 2240 \times 10^3$ ($M_w/M_n = 1.08$) was dissolved in toluene with concentrations of PS ranging from 0.9 to 2.0 % by mass, and then spincoated onto freshly cleaved mica substrates rotating at an angular speed of 4000 rpm. For $M_w = 2240 \times 10^3$, we prepared a series of films with thicknesses of 91 ± 3, 68 ± 1, and 51 ± 1 nm, and for $M_w = 717 \times 10^3$, we prepared a series of films with thicknesses of 97 ± 1 and 54 ± 1 nm. All films were annealed under vacuum at $T = 115$ °C for 12 h after spincoating onto mica substrates and then cooled slowly to room temperature at 1 °C/min. This ensured that trapped solvent molecules were removed, and that the films had a well-defined and reproducible thermal history. A water transfer technique [4] was used to suspend the PS films over a 4 mm circular opening in a stainless steel sample holder. Film thicknesses were determined to within ± 1 nm using ellipsometry on identical PS films that were placed onto Si wafers using the water transfer technique. Prior to each run of the DPE, the freely standing PS films were examined using optical microscopy to ensure that there were no preexisting holes or tears, which would degrade or prevent the DPE measurement.

In the differential pressure experiment (DPE), which was designed and constructed in-house, a very small pressure difference was applied across a freely standing polymer film held at a fixed elevated temperature T. The flow of gas across the freely standing film was monitored by tracking the position x of a piston used in a feedback loop to maintain a small, constant pressure difference across the film. In the following description, we highlight the main features of the DPE; the

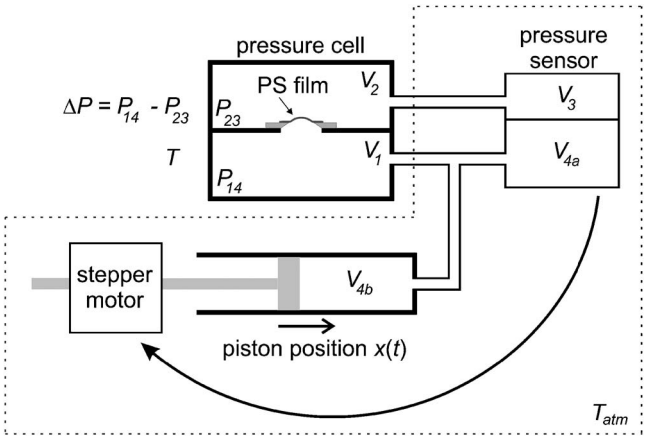

FIG. 1. Schematic diagram of the differential pressure experiment (DPE). See text for the symbol details. (Diagram reproduced with permission from Ref. [27].)

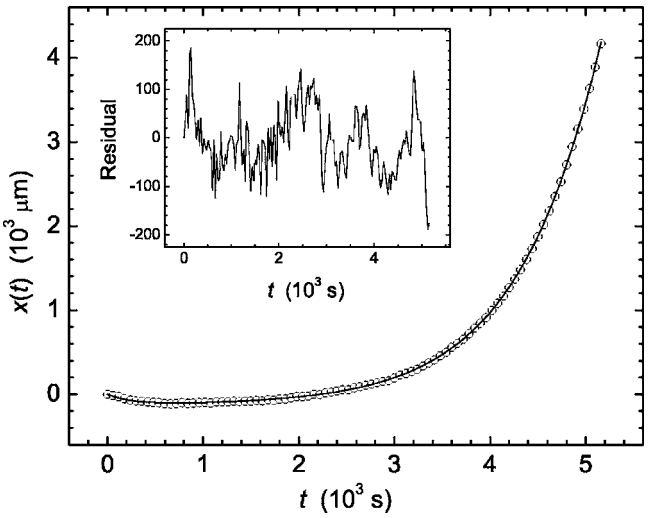

FIG. 2. Piston position x as a function of time t for a freely standing polystyrene (PS) film of $M_w = 2240 \times 10^3$ and $h = 50$ nm measured at $T = 98$ °C. Shown are both the $x(t)$ data (symbols) and a best fit to the data (curve) calculated using Eqs. (5) and (6) with the following parameter values $\tau = 2420 \pm 10$ s, $t_0 = 120$ s, $t_w = 390$ s, $A_1 = 50$ mm, $A_2 = 15$ Pa, $C_0 = 120$ μm, and $t_1 = 240$ s. The residual to the fit [measured $x(t)$ values − calculated $x(t)$ values] is shown in the inset.

complete details of the experimental setup and data analysis are discussed in Ref. [27]. The heart of the DPE is a pressure cell that is divided into two compartments, with volume V_1 at a pressure P_{14} and V_2 at P_{23} (see Fig. 1). The freely standing polymer film is placed over a hole between the two compartments of the pressure cell, forming a barrier between the two volumes V_1 and V_2, and allowing the application of a pressure difference $\Delta P = P_{14} - P_{23}$ across the freely standing polymer film. The pressure difference ΔP is continuously monitored by a differential pressure sensor and maintained using a computer-controlled active feedback loop that determines the position x of the piston. The piston forms part of the volume V_4 and is connected to volume V_1 of the pressure cell, thus actively controlling the pressure in the lower compartment of the cell. Typically a ΔP value of 6.6 Pa $\cong 10^{-4}$ atm was applied across the polymer film. This small pressure difference was chosen to be as small as possible so as to gently bow the film and allow the flow of gas through holes in the film to be detected. We found that doubling ΔP resulted in hole growth times that were indistinguishable from those measured using the lower value of ΔP, indicating that the in-plane stress due to the application of ΔP did not affect the hole growth measurement appreciably.

For the DPE measurement, the sample cell was heated to an elevated temperature T, within the range $92\ ^\circ\text{C} < T < 105\ ^\circ\text{C}$, and it was held constant for each measurement to within $\pm 0.1\ ^\circ$C. In addition, we have found that for long term stability of the experiment, it was necessary to place the volumes V_3 and V_4 within a sealed chamber (see Fig. 1) held at a temperature $T_{atm} \simeq 30\ ^\circ$C that was slightly higher than ambient. Because it was necessary to open the sealed chamber at the beginning of each experiment, a small time-dependent background signal in $x(t)$ was obtained as $T_{atm}(t)$ returned to its setpoint value over a period of approximately 30 min.

As holes in the film form and grow, the piston must continuously drift in one direction (to the right in Fig. 1) to maintain a constant value of ΔP across the film. The piston position $x(t)$ data were fit to the following functional form [27]

$$x(t) = A_1 \times \frac{A_2 G}{P_{14}(0) + A_2 G} - C_0(1 - e^{-t/t_1}), \tag{5}$$

with

$$G = e^{3(t-t_0)/\tau} e^{(3t_w/2\tau)^2} \left[\text{erf}\left(\frac{t - t_0}{t_w} + \frac{3t_w}{2\tau} \right) + \text{erf}\left(\frac{t_0}{t_w} - \frac{3t_w}{2\tau} \right) \right] - \left[\text{erf}\left(\frac{t - t_0}{t_w} \right) + \text{erf}\left(\frac{t_0}{t_w} \right) \right], \tag{6}$$

where "erf" is the standard error function. The right-hand side of Eq. (5) contains two terms: the first term is due to air flow through the holes in the film, all of which are assumed to grow exponentially with the same characteristic growth time τ, and the second term is due to the small background signal caused by the initial time dependence of $T_{atm}(t)$, which is characterized by a time t_1 and an overall scaling constant C_0. Holes form in the films at different times as described by a Gaussian distribution centered on time t_0 with width t_w. A_1 and A_2 are scaling constants and $P_{14}(0)$ is the pressure in volume V_1 and V_4 at the start of the experiment. For a full derivation of Eqs. (5) and (6) and the procedure used to fit the $x(t)$ data, see Ref. [27].

III. RESULTS AND DISCUSSION

The piston position $x(t)$ measured using the DPE for a freely standing PS film of $M_w = 2240 \times 10^3$ and $h = 50$ nm held at $T = 98\ ^\circ$C is shown in Fig. 2. This $x(t)$ data set is representative of all $x(t)$ data sets obtained in the present study: a small negative drift at short times due to the background signal, and a large positive signal at long times indi-

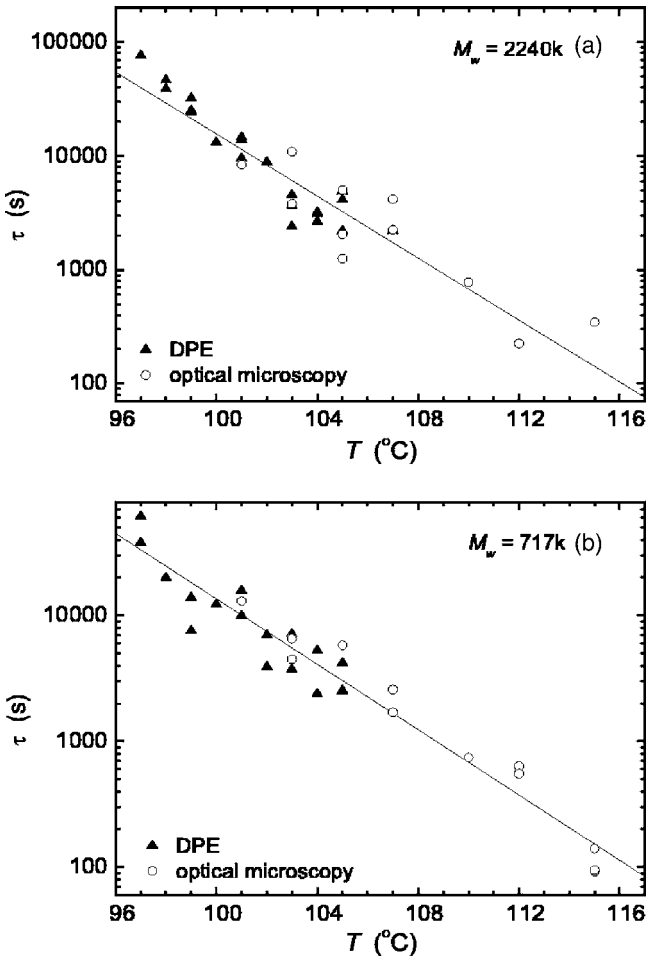

FIG. 3. Comparison of the dependence of the characteristic growth time τ versus temperature T determined using the DPE (▲) and determined using optical microscopy (◯) from Ref. [29]. (a) $M_w=2240\times10^3$: $h=91$ nm from DPE and $h=83$ nm from optical microscopy, (b) $M_w=717\times10^3$: $h=97$ nm from DPE and $h=90$ nm from optical microscopy. The lines correspond to fits of the $\log_{10}\tau$ versus T data to a straight line for all of the data.

cating the growth of holes due to the flow of gas through the film. Equations (5) and (6) were used to fit the $x(t)$ data to obtain the best fit parameter values. The residual to the fit, shown in the inset of Fig. 2, indicates that a very good fit to the data is obtained for all times.

For a given sample, many holes form over the surface area of the film and all of the holes are assumed to grow with the same characteristic growth time τ, as defined in Eq. (1). In Fig. 3 is shown a plot of the best fit values of τ as a function of the measurement temperature T obtained using the DPE for (a) $M_w=2240\times10^3$, $h=91$ nm films and (b) $M_w=717\times10^3$, $h=97$ nm films. The $\tau(T)$ data exhibit a strong temperature dependence as expected, since the growth time τ is directly proportional to viscosity [see Eq. (2)]. Unfortunately the range of temperatures probed in the DPE measurements is too small to distinguish between a Vogel-Fulcher-Taumann (VFT) or Arrhenius temperature dependence. The duration of the DPE measurement at low temperatures is limited to times less than ~48 h due to a small drift in the piston position, and at high temperatures to times greater than ~30 min due to the presence of the background signal. The upper limit on temperature can be increased by using optical microscopy to measure the radius $R(t)$ of individual holes directly [26,29]. Figure 3 also shows $\tau(T)$ values obtained from optical microscopy measurements [29] plotted as open circles for films with the same M_w values and comparable thicknesses: (a) $M_w=2240\times10^3$, $h=83$ nm and (b) $M_w=717\times10^3$, $h=90$ nm. We note there is excellent agreement between τ values obtained from the DPE and those measured using optical microscopy.

In the derivation of Eqs. (5) and (6), the holes are assumed to grow exponentially with time [see Eq. (1)], characterized by a single growth time τ. However, in Ref. [29], in which the time dependence of the radius $R(t)$ of a single hole was measured directly, a transition from linear growth of the hole radius during the early stages of hole growth to exponential growth at later times was observed at low temperatures and high molecular weight values. The $R(t)$ data from Ref. [29] were fit to an expression for exponential growth of the hole radius which is modified to incorporate a time-dependent viscosity $\eta(t)$ resulting in the expression

$$R(t) = R_0 \exp\{t/\tau[1 + \exp(-t/\tau_1)]\}. \quad (7)$$

Equation (7) describes both the exponential growth at long times, with characteristic growth time τ, as well as the transient behavior at short times, which was found to decay on a time scale $\tau_1 \sim \tau/2$ [29]. Although the DPE signal is dominated by gas flow through the largest holes, which are growing exponentially, it is likely that there is also a substantial contribution to the DPE signal from holes that are growing linearly with time, corresponding to the transient behavior. To simplify the data analysis, we have assumed exponential growth of the radius for each hole, allowing us to obtain values of τ. The results shown in Fig. 3 demonstrate that the τ values obtained from the DPE, assuming exponential growth, are in agreement to within the reproducibility of the τ values with the τ values determined from optical microscopy measurements of $R(t)$ in the limit of long times for which exponential growth is observed.

In Fig. 4 are shown the $\tau(T)$ values measured for films with $M_w=2240\times10^3$ and three different film thickness values $h=91$, 68, and 51 nm. The lines are best fits to the $\log_{10}\tau$ versus T data for each nominal film thickness. There is a distinct shift between each of the three data sets in Fig. 4, but the shifts are small. For example, shifts in temperature of only a few degrees Celsius are necessary to to make one data set coincide with another data set: 2.4 °C shift between the $h=91$ and 68 nm data, and 4.7 °C shift between the $h=91$ and 51 nm data. The small temperature shifts between the different data sets are quite surprising because the T_g values corresponding to these three film thicknesses are markedly different: $T_g=97$ °C (the bulk value) for $h=91$ nm, $T_g=67$ °C for $h=68$ nm, and $T_g=25$ °C for $h=51$ nm [5]. In bulk polymers, segmental and whole chain motion have the same temperature dependence, a property that is referred to as time-temperature superposition. Consequently, we might expect the DPE data corresponding to smaller thickness values to be shifted down in temperature by an amount compa-

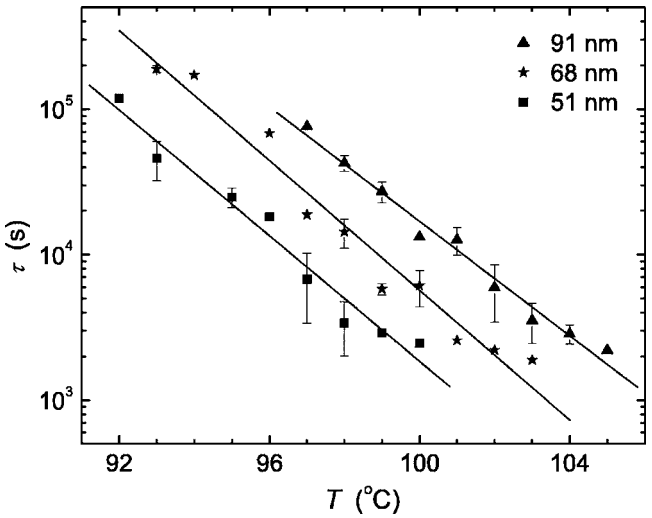

FIG. 4. Characteristic growth time τ of the holes plotted as a function of the measurement temperature T for all of the freely standing PS films of $M_w=2240\times10^3$ measured using the DPE: $h=91$ nm (▲), $h=68$ nm (★), and $h=51$ nm (■). The lines correspond to fits of the $\log_{10}\tau$ versus T data to a straight line for data obtained for each nominal film thickness.

rable to the reduction in T_g, i.e., many tens of degrees Celsius. However, hole formation and growth occurs at comparable temperatures with comparable characteristic times for all of the films in the present study. As a result, we find that very thin freely standing PS films with reduced values of T_g are stable to the formation of holes at temperatures that are tens of degrees Celsius greater than the T_g value of the film.

In Fig. 5 is shown $\tau(T)$ data for $M_w=717\times10^3$ freely standing PS films with $h=97$ and 54 nm; and $M_w=2240\times10^3$ freely standing PS films with $h=91$ and 51 nm. We can clearly see that there is no measurable dependence of the

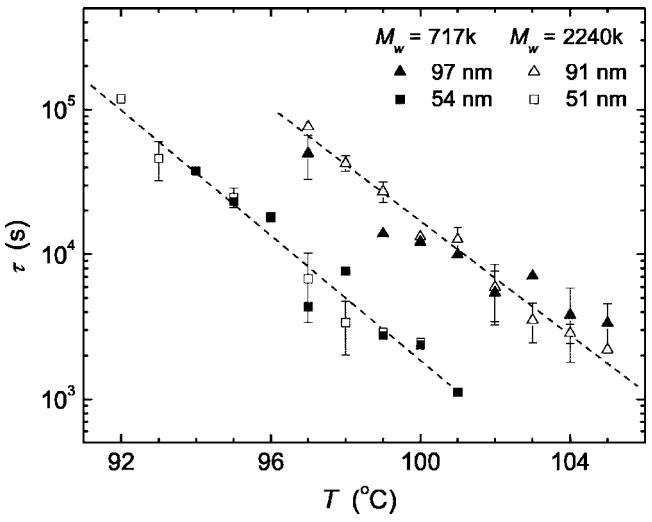

FIG. 5. $\tau(T)$ data measured using the DPE for freely standing PS films of $M_w=717\times10^3$ with $h=97$ nm (▲) and $h=54$ nm (■); and $M_w=2240\times10^3$ with $h=91$ nm (△) and $h=51$ nm (□). The lines correspond to fits of the $\log_{10}\tau$ versus T data to a straight line for films with $M_w=2240\times10^3$.

$\tau(T)$ values on M_w, which is consistent with the lack of dependence of the viscosity on M_w in the shear thinning regime [43]. The films with $M_w=717\times10^3$ show the same small shift (4.7 °C) between the data sets for the two film thickness values as that observed between the data sets for two comparable film thickness values for films with $M_w=2240\times10^3$ even though the difference in T_g values for the two film thicknesses is much smaller for the films with $M_w=717\times10^3$ (28 °C difference in T_g between the $h=97$ and 54 nm films).

In Figs. 4 and 5 are shown τ values obtained from hole growth measurements both above and below the bulk value of $T_g^{\text{bulk}}=97$ °C for PS. We found that holes formed in the films at temperatures below T_g^{bulk} only for films which had reduced values of T_g. The lowest temperature for which hole growth was observed was $T=92$ °C, which is 5 °C below T_g^{bulk}, for a very thin film ($h=51$ nm, $M_w=2240\times10^3$) which had the lowest value of $T_g=25$ °C. We find that the τ values measured for temperatures below T_g^{bulk} are consistent with values extrapolated from temperatures greater than T_g^{bulk} using a fit of the $\log_{10}\tau$ versus T data. Although hole formation and growth was observed at temperatures below T_g^{bulk} for films with reduced values of T_g, these temperatures were only slightly less than T_g^{bulk} and the growth times τ were found to be comparable for both thick and thin films. As discussed in Ref. [29], even though the reptation time τ_d is very long at temperatures comparable to T_g^{bulk}, chains can disentangle over time scales less than τ_d at high shear strain rates via other relaxation mechanisms, such as the convective constraint release (CCR) mechanism [48].

We can account for the small shifts between the $\tau(T)$ data sets of Figs. 4 and 5 by considering the shear thinning phenomenon [35,36]. For hole growth in thin polymer films, a larger stress $\sigma=2\epsilon/h$ is obtained at the edge of the hole for a smaller value of h, which produces an increase in the shear strain rate $\dot{\gamma}$ and a corresponding decrease in η [see Eq. (4)]. A plot of the ratio of the viscosity η at the edge of the hole to the zero strain rate viscosity η_0 versus the reduced shear strain rate

$$\beta=\frac{\eta_0 M_w\dot{\gamma}}{\rho R_{\text{mol}}T} \tag{8}$$

is shown in part (a) of Fig. 6 for the data collected in the present study. The use of the β parameter results in the overlay of data collected at different temperatures T, molecular weights M_w, and thicknesses h. In Eq. (8), R_{mol} is the molar gas constant and ρ is the mass density of PS. In part (a) of Fig. 6, the value of d [see Eq. (4)] used to calculate the best fit straight line to the $\log_{10}(\eta/\eta_0)$ versus β data was 0.77 ± 0.01, which is in excellent agreement with the value of 0.75 ± 0.01 obtained in recent optical microscopy measurements of freely standing PS films [29]. In part (b) of Fig. 6, we have plotted η/η_0 versus β for all of the available hole growth data for freely standing PS films obtained for both optical microscopy and DPE measurements, including the present study [26–29], and the value of d used to calculate the best fit straight line to the $\log_{10}(\eta/\eta_0)$ versus β data for Refs. [26,27,29] and the present study was 0.78 ± 0.01.

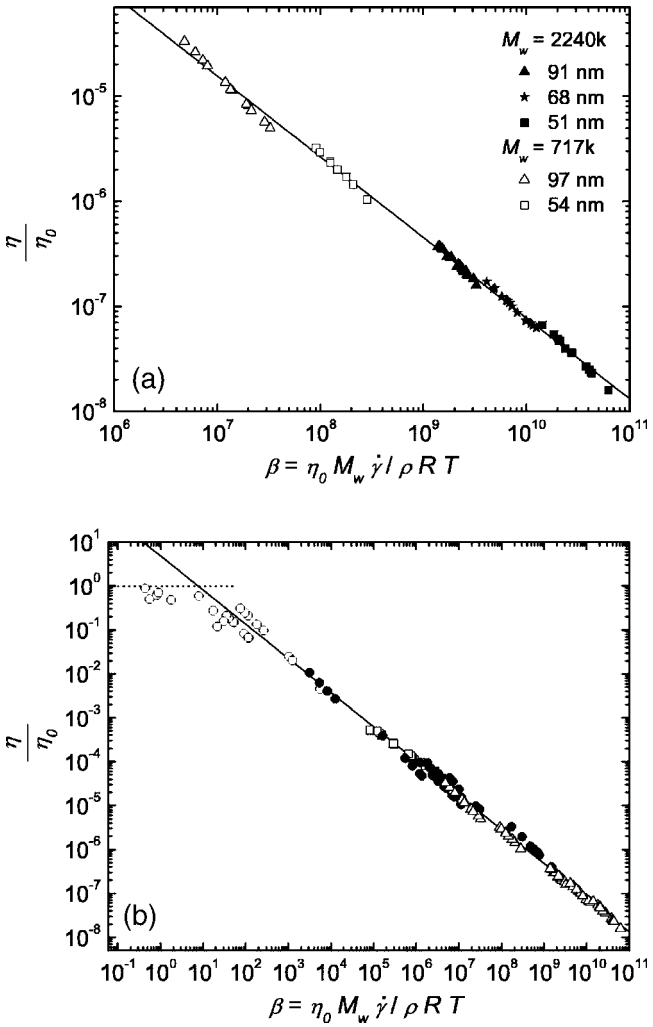

FIG. 6. (a) Viscosity η at the edge of the hole, normalized to the zero shear rate viscosity η_0, as a function of the reduced strain rate β for all of the τ values from Figs. 4 and 5. The symbols for the freely standing PS film data of $M_w = 2240 \times 10^3$ are $h = 91$ nm (▲), $h = 68$ nm (★), and $h = 51$ nm (■); and $M_w = 717 \times 10^3$ are $h = 97$ nm (△) and $h = 54$ nm (□). The slope of the best fit line through all of the data is -0.77 ± 0.01. (b) Viscosity η at the edge of the hole, normalized to the zero shear rate viscosity η_0, as a function of the reduced strain rate β for the DPE (△) and all of the optical microscopy [data from Ref. [29] (●), Ref. [26] (□) and Ref. [28] (◯)] studies of hole growth in freely standing PS films [26–29]. The slope of the best fit line through all of the data represented by the ● and △ symbols is -0.78 ± 0.01.

Where there is overlap of the β values in the different studies, there is excellent agreement between the corresponding η/η_0 values. It is interesting to note that the data of Ref. [28], obtained for thicker films at higher temperatures than in the present study, extend the range of the data in Fig. 6 from the nonlinear regime to the linear regime, corresponding to $\eta = \eta_0$, indicating that hole growth is a shear deformation and not an extensional deformation since the steady state extensional viscosity at small strain rates, the Trouton viscosity, is three times the zero shear viscosity η_0. The combined data shown in part (b) of Fig. 6, which extend over almost 12 orders of magnitude in β and correspond to reductions in

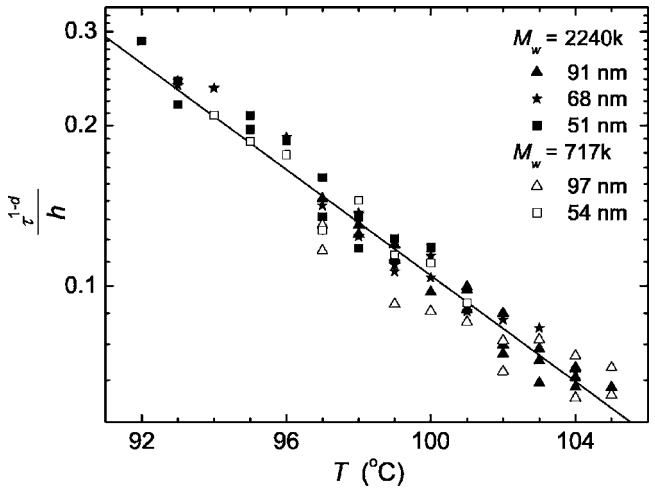

FIG. 7. τ^{1-d}/h versus T, with $d = 0.77$, for all of the data collected with the DPE for freely standing PS films of $M_w = 2240 \times 10^3$: $h = 91$ nm (▲), $h = 68$ nm (★), and $h = 51$ nm (■); and $M_w = 717 \times 10^3$: $h = 97$ nm (△) and $h = 54$ nm (□). The line is a best fit straight line to all of the data.

η/η_0 of up to 8 orders of magnitude, strongly suggest that the hole growth process in thin freely standing PS films at temperatures comparable to T_g^{bulk} corresponds to viscous flow, with a reduced viscosity due to shear thinning, for the times and temperatures for which exponential growth is observed.

The data shown in Fig. 6 were calculated using the following procedure. The value of η at the edge of the hole was obtained from the measured value of τ using Eq. (2), where the values for the surface tension ϵ of PS were calculated at different temperatures T using the equation [49]

$$\epsilon = -0.072(T - 20) + 40.7, \tag{9}$$

with ϵ in mN/m for T in degrees Celsius. The η_0 values at each temperature T and M_w were determined from the value of $\eta_0 = 1.2 \times 10^{11}$ Pa s measured at $T = 119.4$ °C for PS of $M_w = 600 \times 10^3$ [50], and scaled using $\eta_0 \sim M_w^{3.4}$ and the VFT equation

$$\eta_0(T) = A \exp\left(\frac{T_A}{T - T_0}\right), \tag{10}$$

with parameters $T_A = 2022$ K and $T_0 = 311$ K obtained from viscosity measurements of high M_w PS [50,51]. To calculate the reduced shear strain rate β values [Eq. (8)], the shear strain rate $\dot{\gamma}$ was calculated using Eq. (3). Values for the density ρ of PS at a given temperature T were calculated using the equation [52,53]

$$\rho = 1.0865 - 6.19 \times 10^{-4} T + 0.136 \times 10^{-6} T^2, \tag{11}$$

with ρ in g/cm^3 for T in degrees Celsius.

To account for the shifts between the $\tau(T)$ data sets of Figs. 4 and 5 due to differences in the degree of shear thinning caused by differences in film thickness h, we plot $(\tau^{1-d})/h$ versus temperature T in Fig. 7. In this plot, all of the data obtained for films with different h and M_w values collapse onto a single line, yielding a universal scaling plot of

the data. We can see that the quantity $(\tau^{1-d})/h$ is independent of M_w by combining Eqs. (2), (3), and (4) to obtain

$$\frac{\tau^{1-d}}{h} = \frac{\eta_0 \dot{\gamma}_{\mathrm{cr}}^d}{2^d \epsilon}, \tag{12}$$

and noting that the product $\eta_0 \dot{\gamma}_{\mathrm{cr}}^d$, as specified in Eq. (4), is independent of M_w since $\eta(\dot{\gamma})$ is independent of M_w in the shear thinning regime, as described in the Introduction [43]. The universal scaling plot of the $\tau(T)$ data shown in Fig. 7 suggests that the small shifts between the different data sets with different h in Figs. 4 and 5 are likely due to shear thinning caused by the increased stress at the edge of the holes in the thinner films.

We distinguish between two aspects of hole formation and growth in freely standing PS films: the dependence on temperature of the characteristic time τ for hole growth, as discussed above, and the onset temperature for the formation of holes. Since holes form in the films at different times, which depends on the density of nucleation sites within the films, it is difficult to comment quantitatively on the onset temperature for hole formation. However, an indication of differences in the onset temperatures for hole formation can be obtained from a plot of the temperature dependence of the best fit average onset times t_0 obtained from fits of Eq. (5) to the $x(t)$ data as shown in Fig. 8. By comparing the temperatures corresponding to a specific value of t_0 for the different data sets, we can see that holes form more readily at lower temperatures in thinner films. Specifically, hole formation was observed only for temperatures equal to or greater than T_g^{bulk} for thicker films with $T_g = T_g^{\mathrm{bulk}}$, whereas hole formation was observed for temperatures slightly less than T_g^{bulk} for thinner films with reduced values of T_g. Therefore there is a trend to lower onset temperature for films with lower values of T_g, but the reduction in onset temperature is independent of M_w (see Fig. 8) and is roughly an order of magnitude smaller than the reduction in T_g. This suggests that the reduction in onset temperature for thinner films may be determined primarily by the reduction in the critical radius for nucleation $R_c = h/2$ and not by the reduction in T_g.

The dramatic difference between T_g and the temperature at which substantial hole formation and growth occurs upon heating of the films is one of the most striking results of the present study. The discrepancy in temperatures can be explained by several possible effects: variation in mobility across the thickness of the film, difference in mobility parallel to and perpendicular to the plane of the film, and the decoupling of segmental and chain motion in very thin polymer films. Since the formation of a hole in the film requires the motion of chains across the entire thickness of the film, hole growth will therefore be limited by the slowest segments of the chains. It is possible that there is a variation in mobility across the thickness of the film, with more mobile segments near the free surface, as inferred from other experiments (for a recent review of this issue, see Ref. [2]). The apparent contradiction could also be explained by large differences in the polymer mobility parallel and perpendicular to the film. Formation of a hole requires motion of entire chains perpendicular to the plane of the film, whereas motion could be enhanced parallel to the plane of the film and suppressed perpendicular to the plane of the film, as suggested by computer simulations [54–58]. The decoupling of segmental and chain motions in thin polymer films has implications for time-temperature superposition, which refers to the equivalence of a shift in temperature and a shift in time, that is found to hold rather well in bulk [59]. However, in thin films, the temperature dependence of the two types of motion might not be the same. This might occur if motions greater than some length scale comparable to the overall size of the molecules are suppressed at temperatures comparable to T_g in very thin polymer films, which is consistent with the experimentally observed decrease in contrast of the thermal expansion of the glass and melt with decreasing film thickness [60]. The current situation is that there are several possible explanations, but not definite resolution, for this issue, and it highlights the importance of understanding the nature of the mobility being probed in a given experiment so that meaningful comparisons of the results of different experimental studies can be made.

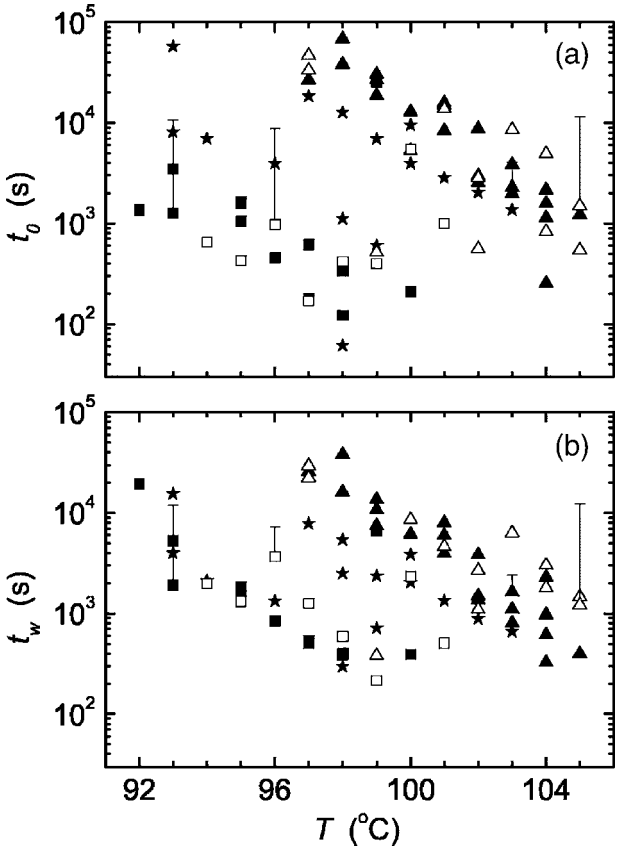

FIG. 8. Best fit values of the (a) t_0 and (b) t_w parameters which describe the Gaussian distribution of onset times centered on time t_0 with width t_w used to model hole formation in the derivation of Eq. (6). Data are shown for all of the freely standing PS films with $M_w = 2240 \times 10^3$: $h = 91$ nm (▲), $h = 68$ nm (★), and $h = 51$ nm (■); and $M_w = 717 \times 10^3$: $h = 97$ nm (△) and $h = 54$ nm (□). Representative error bars (positive-going only) are given for several data sets; each error bar represents the average of the uncertainties of the best fit values for that data set.

IV. CONCLUSIONS

We have used a differential pressure experiment (DPE) to measure the growth time τ of holes in thin freely standing polystyrene films with $M_w = 717 \times 10^3$ and 2240×10^3, for films with thicknesses from $h = 51$ to 97 nm for which reductions in the glass transition temperature T_g were previously observed using ellipsometry. $\tau(T)$ values were measured at temperatures close to the bulk value of the glass transition temperature T_g^{bulk}, and found to be comparable for all films despite the large differences in T_g between the thinner and thicker films. The small shifts in the $\tau(T)$ values with h were explained quantitatively by the shear thinning mechanism. Several possible explanations for the large difference between the temperature at which substantial hole formation and growth occurs upon heating of very thin films and the T_g values measured for those films were proposed.

ACKNOWLEDGMENTS

Financial support of the Natural Sciences and Engineering Research Council (NSERC) of Canada and the Province of Ontario (PREA program) is gratefully acknowledged.

[1] J. A. Forrest and K. Dalnoki-Veress, Adv. Colloid Interface Sci. **94**, 167 (2001).
[2] C. B. Roth and J. R. Dutcher, in *Soft Materials: Structure and Dynamics*, edited by J. R. Dutcher and A. G. Marangoni (Marcel Dekker, New York, 2004).
[3] J. A. Forrest, K. Dalnoki-Veress, J. R. Stevens, and J. R. Dutcher, Phys. Rev. Lett. **77**, 2002 (1996); **77**, 4108 (1996).
[4] J. A. Forrest, K. Dalnoki-Veress, and J. R. Dutcher, Phys. Rev. E **56**, 5705 (1997).
[5] K. Dalnoki-Veress, J. A. Forrest, C. Murray, C. Gigault, and J. R. Dutcher, Phys. Rev. E **63**, 031801 (2001).
[6] J. Mattsson, J. A. Forrest, and L. Börjesson, Phys. Rev. E **62**, 5187 (2000).
[7] C. B. Roth and J. R. Dutcher, Eur. Phys. J. E **12**, 024 (2003).
[8] B. Frank, A. P. Gast, T. P. Russell, H. R. Brown, and C. Hawker, Macromolecules **29**, 6531 (1996).
[9] X. Zheng, M. H. Rafailovich, J. Sokolov, Y. Strzhemechny, S. A. Schwarz, B. B. Sauer, and M. Rubinstein, Phys. Rev. Lett. **79**, 241 (1997).
[10] Y. Pu, M. H. Rafailovich, J. Sokolov, D. Gersappe, T. Peterson, W.-L. Wu, and S. A. Schwarz, Phys. Rev. Lett. **87**, 206101 (2001).
[11] Y. Pu, H. White, M. H. Rafailovich, J. Sokolov, A. Patel, C. White, W.-L. Wu, V. Zaitsev, and S. A. Schwarz, Macromolecules **34**, 8518 (2001).
[12] T. Kuhlmann, J. Kraus, P. Müller-Buschbaum, D. W. Schubert, and M. Stamm, J. Non-Cryst. Solids **235–237**, 457 (1998).
[13] J. A. Forrest and K. Dalnoki-Veress, J. Polym. Sci., Part B: Polym. Phys. **39**, 2664 (2001).
[14] D. Kawaguchi, K. Tanaka, T. Kajiyama, A. Takahara, and S. Tasaki, Macromolecules **36**, 1235 (2003).
[15] G. Reiter, Macromolecules **27**, 3046 (1994).
[16] T. G. Stange, D. F. Evans, and W. A. Hendrickson, Langmuir **13**, 4459 (1997).
[17] R. Seemann, S. Herminghaus, and K. Jacobs, Phys. Rev. Lett. **87**, 196101 (2001).
[18] J.-L. Masson and P. F. Green, Phys. Rev. Lett. **88**, 205504 (2002).
[19] J.-L. Masson and P. F. Green, Phys. Rev. E **65**, 031806 (2002).
[20] G. Reiter, Phys. Rev. Lett. **87**, 186101 (2001).
[21] G. Reiter, Eur. Phys. J. E **8**, 251 (2002).
[22] G. Reiter, M. Sferrazza, and P. Damman, Eur. Phys. J. E **12**, 133 (2003).
[23] P. Damman, N. Baudelet, and G. Reiter, Phys. Rev. Lett. **91**, 216101 (2003).
[24] G. Debrégeas, P. Martin, and F. Brochard-Wyart, Phys. Rev. Lett. **75**, 3886 (1995).
[25] G. Debrégeas, P.-G. de Gennes, and F. Brochard-Wyart, Science **279**, 1704 (1998).
[26] K. Dalnoki-Veress, B. G. Nickel, C. Roth, and J. R. Dutcher, Phys. Rev. E **59**, 2153 (1999).
[27] C. B. Roth, B. G. Nickel, J. R. Dutcher, and K. Dalnoki-Veress, Rev. Sci. Instrum. **74**, 2796 (2003).
[28] J. H. Xavier, Y. Pu, C. Li, M. H. Rafailovich, and J. Sokolov, Macromolecules **37**, 1470 (2004).
[29] C. B. Roth, B. Deh, B. G. Nickel, and J. R. Dutcher, the preceding paper, Phys. Rev. E **72**, 021802 (2005).
[30] K. C. Tseng, N. J. Turro, and C. J. Durning, Phys. Rev. E **61**, 1800 (2000).
[31] D. B. Hall and J. M. Torkelson, Macromolecules **31**, 8817 (1998).
[32] Y. M. Boiko and R. E. Prud'homme, J. Polym. Sci., Part B: Polym. Phys. **36**, 567 (1998).
[33] J. N. Israelachvili, *Intermolecular & Surface Forces*, 2nd ed. (Academic, San Diego, 1991).
[34] J. D. Gunton, M. S. Miguel, and P. S. Sahni, in *Phase Transitions and Critical Phenomena*, edited by C. Domb and J. L. Lebowitz (Academic Press, London, 1983), Vol. 8.
[35] W. W. Graessley, Adv. Polym. Sci. **16**, 1 (1974).
[36] R. B. Bird, C. Curtiss, R. Armstrong, and O. Hassager, *Dynamics of Polymeric Liquids* (Wiley, New York, 1987), Vol. 1.
[37] L. Bergström, Colloids Surf., A **133**, 151 (1998).
[38] J. Bergenholtz, Curr. Opin. Colloid Interface Sci. **6**, 484 (2001).
[39] H. Watanabe, Acta Polym. **48**, 215 (1997).
[40] G. G. Fuller, Curr. Opin. Colloid Interface Sci. **2**, 153 (1997).
[41] H. A. Nasreldin, Adv. Chem. Ser. **231**, 171 (1992).
[42] A. Peterlin, Adv. Macromol. Chem. **1**, 225 (1968).
[43] R. A. Stratton, J. Colloid Interface Sci. **22**, 517 (1966).
[44] F. Saulnier, E. Raphaël, and P.-G. de Gennes, Phys. Rev. Lett. **88**, 196101 (2002).
[45] F. Saulnier, E. Raphaël, and P.-G. de Gennes, Phys. Rev. E **66**, 061607 (2002).
[46] V. Shenoy and A. Sharma, Phys. Rev. Lett. **88**, 236101 (2002).
[47] S. Herminghaus, R. Seemann, and K. Jacobs, Phys. Rev. Lett. **89**, 056101 (2002).
[48] T. C. B. McLeish, Adv. Phys. **51**, 1379 (2002).
[49] *Polymer Handbook*, edited by J. Brandrup and E. H. Immer-

gut, 3rd ed. (Wiley, New York, 1989).
[50] D. J. Plazek and V. M. O'Rourke, J. Polym. Sci., Part A-2 **9**, 209 (1971).
[51] K. L. Ngai and D. J. Plazek, in *Physical Properties of Polymers Handbook*, edited by J. E. Mark (AIP, Woodbury, NY, 1996), Chap. 25.
[52] R. A. Orwoll, in *Physical Properties of Polymers Handbook*, edited by J. E. Mark (AIP, Woodbury, NY, 1996), Chap. 7.
[53] H. Höcker, G. J. Blake, and P. J. Flory, Trans. Faraday Soc. **67**, 2251 (1971).
[54] J. Baschnagel and K. Binder, J. Phys. I **6**, 1271 (1996).
[55] K. F. Mansfield and D. N. Theodorou, Macromolecules **22**, 3143 (1989).
[56] I. Bitsanis and G. Hadziioannau, J. Chem. Phys. **92**, 3827 (1990).
[57] T. Matsuda, G. D. Smith, R. G. Winkler, and D. Y. Yoon, Macromolecules **28**, 165 (1995).
[58] P. Doruker and W. L. Mattice, Macromolecules **32**, 194 (1999).
[59] K. L. Ngai and D. J. Plazek, Rubber Chem. Technol. **68**, 376 (1995).
[60] J. A. Forrest, J. Mattsson, and L. Börjesson, Eur. Phys. J. E **8**, 129 (2002).